IEEE Access
Multidisciplinary | Rapid Review | Open Access Journal

Received January 18, 2020, accepted January 31, 2020, date of publication February 10, 2020, date of current version February 18, 2020.

Digital Object Identifier 10.1109/ACCESS.2020.2972648

Communication Network for Ultrasonic Acoustic Water Leakage Detectors

AMEEN AWWAD[1], MOHAMED YAHYIA[2], LUTFI ALBASHA[1], MD. MARUF MORTULA[3], AND TARIG ALI[2]

[1]Electrical Engineering Department, American University of Sharjah, Sharjah 26666, United Arab Emirates
[2]GIS and Mapping Laboratory, American University of Sharjah, Sharjah 26666, United Arab Emirates
[3]Civil Engineering Department, American University of Sharjah, Sharjah 26666, United Arab Emirates

Corresponding author: Ameen Awwad (b00055027@alumni.aus.edu)

This work was supported by the Smart City Research Institute Grant at the American University of Sharjah, United Arab Emirates, under Grant EN-0282.

ABSTRACT Water leaks in the distribution network produce significant losses and cause serious economic inconvenience especially in areas with water shortage. In this paper, the operational aspects of the most popular offline detection technologies, ground penetrating radars (GPR's), infrared (IR) cameras, and acoustic detectors, were compared. The authors also studied the potential of using the recent Terahertz imaging technology for the same application. Acoustic detectors were found the most suitable technology for the atmosphere in UAE, where the levels of humidity and, consequently, soil moisture are high, because both of GPRs and IR cameras operational capability to detect leaks tend to decrease sharply as soil moisture increases. On the other side, a conventional acoustic detector has very limited scope of detection. This paper presents a method of expanding the sensing component of acoustic detectors by connecting acoustic sensors through a digital communication system using the 3G/4G networks to a monitoring center with an acoustic spectrum analyzer. The novelty of this system is its ability to provide offline detection of leakages in the underground water pipelines remotely without deforming the surrounding environment or adjusting the acoustic detector's analyzing system. Simulation results proves the ability of the system to reconstruct the input noise signal at the end of the proposed network which is to be connected to the acoustic analyzer.

INDEX TERMS Water leakage detection, acoustic detector, moisture, ultrasonic noise, frequency conversion, signal sampling, audio recording.

I. INTRODUCTION

Methods of leakage detection in a water distribution system (WDS) include online and offline techniques. Online techniques require sensors to be mounted on or very close to the pipeline, sometimes via access points on the ground level to underground pipes, while offline ones can detect water leaking from underground pipes remotely above the surface. Offline techniques' remote sensing advantage allows inspection without destructing the underground pipeline structure or the environment round it. The most popular offline detection technologies are ground penetrating radars (GPRs), infrared (IR) cameras, and acoustic detectors [1]. A GPR uses high-frequency radio waves to identify sub-surface's material and image underground physical deformations. It differentiates between different materials by measuring their different reflectivity and measures the depth by recording the travel time and power of the reflected signals to build contour maps. The performance of a GPR is limited by its radiated power and electromagnetic path attenuation in the subsurface. Recently, GPRs were used to detect WDSs' leakage in different surfaces and found capable of imaging the evolution levels of a leakage [1]. However, the readings of a GPR can largely be confused by the moisture in the ground [2]. Additionally, to image a leakage, a GPR must be located exactly above it and to produce a 3D image of the volume of water leaked, the GPR must pass along the volume to be imaged capturing many 2D slices of the subsurface and then combine them to form a 3D image. Fig. 1 shows a raw 2D slice captured by a 1.5 GHz GPR of an underground water leakage and a 3D processed image formed by combining many of these 2D slices. Secondly, IR cameras,

The associate editor coordinating the review of this manuscript and approving it for publication was Yulei Wu.

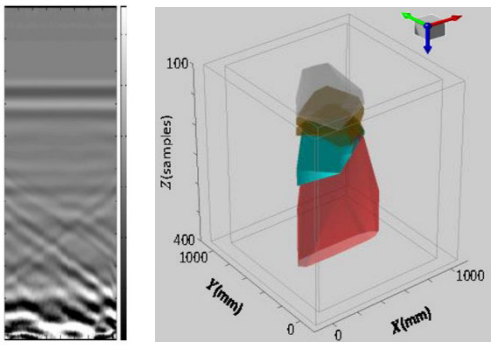

FIGURE 1. (a) A raw 2D slice captured by a 1.5 GHz GPR of a water leakage from a plastic pipe buried in a tank filled with sand (b) a 3D image formed by combining many processed 2D slices [1].

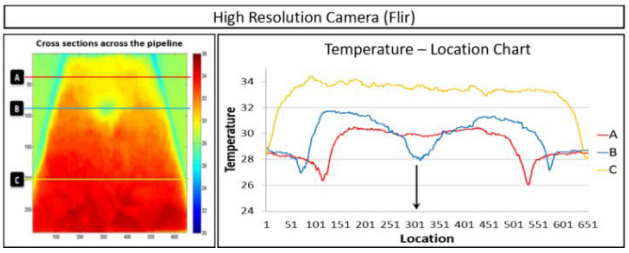

FIGURE 2. A high-resolution IR image of a surface above a simulated underground leakage and the associated temperature profiles [3].

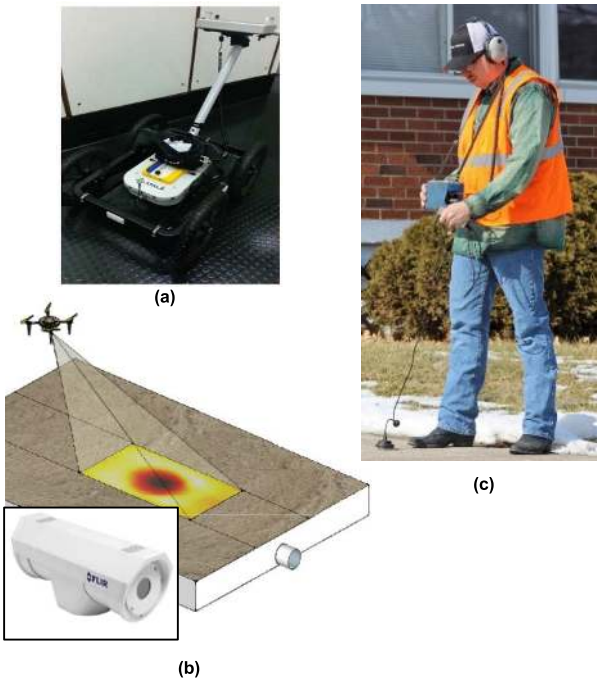

FIGURE 3. Most popular devices that were used in leakage detection: (a) GPR [10]. (b) IR Camera with a model proposing attaching it to a drone [3] (Note that a drone with an integrated IR camera is currently commercially available [11]). (c) Acoustic Detector (An acoustic sensor is placed on the ground and connected to an analyzer held by a worker to process and analyze the received signal and display. The speakers placed on the user's head allow for the listening to ultrasounds converted to audio [12].

thermographic devices that detect infrared radiation of bodies, rely on the change in the temperature of the surface above water leaked which rises by capillarity through the subsurface [3]. Fig. 2 shows a processed IR image of a thermal anomaly on a surface caused by a leakage from a pipeline buried at a depth of 110 mm. According to the profile in Fig. 2, the difference between the temperature directly above the location of the leakage and horizontally adjacent points was about 4 °C.

Currently, the Terahertz (THz) band, which lies between the end of the infrared band and the start of the microwave band, is used in imaging bodies under dielectric surfaces [4]. Like microwave radiation, THz radiation can penetrate a wide variety of non-metallic and non-polar materials, such as plastics, glasses, woods and dry soil, making it suitable for detecting buried objects and concealed illegal materials and underground imaging [4], [5]. The limitation of THz propagation through water enables measuring and imaging moisture faction in other materials and water diffusion using different dielectric models [5]. These models suppose moisture as particles in a host dielectric material and estimates water faction based on the measured constants, like the Effective Absorption (Net Attenuation) Coefficient and Effective Permittivity of the mixture, water particles and the host material, compared mathematically to the known individual constants of each of these materials [6]. However, the measurement of moisture percentage using Absorption Coefficient comparison method was found to be applicable until moisture level reaches 10% where the coefficient starts to increase steeply [6]. Utilizing this system, water content distribution in a host medium can be detected as well, where the deeper the water is in a layer the lower the power of the reflected signal as its range of propagation increases increasing the path attenuation. This reflective approach is suggested to optically test thick samples. To sum up, THz technology has a potential not only to detect leakage in pipelines but to monitor its leaked water path as well. The immature technology of THz radiation suffers from several serious drawbacks. One significant drawback is that the equipment needed to detect this radiation is bulky and expensive [7]. For example, a THz Air-Coupled Time Domain Measurement Kit (ACMK-F), which can test only small pieces of thin samples, such as a multilayer plastic sheet, has a price of $ 89,000 [8]. That high cost of THz equipment is due to the fact that the THz band is considered to be a gap in the electromagnetic spectrum, where at its high-frequency boundary most coherent photonic devices cease to radiate, and at its low-frequency boundary internal losses of electronic oscillators reduce the output power to an insignificant level [9]. Fig. 4 shows a picture of a bulky THz radar, which can be compared to the size of devices used in leakage detection, shown in Fig. 3. Another important drawback is poor images' quality. Poor THz image reconstruction results mainly from the lack of suitable reconstruction algorithms and signal interpretation at that high frequency [14]. Therefore, utilizing THz devices for leakage detection is inefficient technically and economically, especially in the

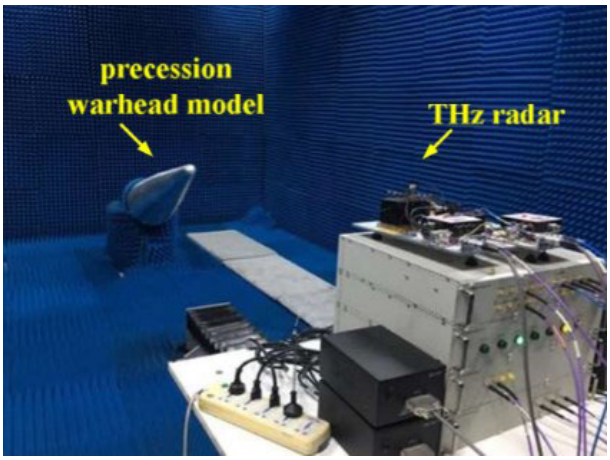

FIGURE 4. THz Radar [13].

existence of other commercially available solutions, such as IR and GPRs, which have moderate prices. Finally, acoustic detectors sense leakage and process the noise produced by streaming water using geophones or microphones by complex mathematical analysis. An acoustic detector usually has a frequency range between 20 and 100 kHz [15], and it incorporates complex filtering system were lots of high-intensity electromagnetic and ultrasonic sources in the environment produce frequencies in this band, such as the electromagnetic radiation produced by fluorescent lighting systems and ultrasonic waves produced by animals, such bats and rodents, and computer and ventilation fans [16]. However, the leakage noise has some distinct characteristics, such as consistent amplitude over time, that facilitate signal processing [17]. Some acoustic detectors' analyzers transform ultrasonic waves into audible sound and its screen displays a frequency and power indictors that go to high levels when a leakage is detected, see Fig. 3 (c) [17]. Additionally, acoustic detectors transform ultrasonic waves into audible sound helping the user to locate the leakage location by comparing the amplitude of sounds produced along the surface above the pipeline. Unlike online acoustic detectors, which are mounted on the pipelines via access points of the WDS [18], offline ones can detect leakage only when it is very close to the surface above it and is used manually to scan the area of interest as shown in Fig. 3 (c). Although a traditional offline acoustic detector is the cheapest device relative to other devices mentioned earlier, it has a limited effective detection scope (e.g. a detector can detect a leakage at a depth of 5 m, but the point on the surface above the leak point must be 0.5 m away from the geophone in average) [18]. Thus, the scope of the sensor of this leakage detection system needs to be expanded to be suitable for a- large monitoring system that can cover a WDS of a city.

II. SPECIFICATIONS AND REQUIREMENTS

Since the moisture percentage in dry soils significantly depends on air humidity [19] (in UAE, air humidity can reach high levels, up to 85 percent [20]), offline acoustic detectors seem to be the best system among the previously mentioned offline leakage detection technologies where its output is not expected to be affected by high moisture levels as there is only a low negative correlation between the sound speed in soil and its water content [21]. To expand the detection scope of that system, it foremost must be divided into two parts: first, data acquisition, and, second, data processing and analysis. Then, the first stage, as it has a single component (acoustic sensor) and consequently a lower cost than the second stage. Multiple sensors placed along the path of a pipeline can transmit data to a single processing and analysis unit. A similar system is already commercially available, where acoustic signals from multiple acoustic sensors distributed along a pipeline are sent to a cloud network where it is processed and analyzed by a single data processing and analysis unit [17]. However, this system is only useful when access to the pipeline structure is permissible [17], unlike the system proposed in this paper, where an offline geophone or other acoustic transducer is used above the subsurface covering the underground pipeline. Table 1 summarizes the aspects of the proposed system, stated at the end of the table, and other devices that can be used in leakage detection mentioned earlier in the previous two sections. To sum up, the objective of this study is to propose a communication network that can connect a data acquisition unit to an analyzer wirelessly with minimal effect on the transmitted ultrasonic signal. This system should be helpful in connecting multiple sensors distributed along the water distribution network (WDN) to a cloud storage. The structure and testing mechanism of such a system is discussed in the next sections.

III. RESEARCH METHODOLOGY

At the beginning of this study, a primary research was conducted about the most popular leakage detection techniques and subsurface imaging technologies. By considering the environmental conditions in the UAE and available communications networks, an integrated system that can sense the ultrasonic noise of water leaks, if there any, all over the water pipeline of SEWA and transfer the acquired data to a data base in the monitoring center to be analyzed was proposed. A MATLAB-based simplified model of the proposed system was used to test its response to a number of ultrasonic signals taking in consideration the acceptable Singla-to-Noise Ratio for data analysis. In the first phase of simulations, the input consists of only two impulses at two ultrasonic frequencies in a certain frequency frame, to be discussed in the next section, to allow a convenient manipulation of the system's parameters. After that, a simulated leakage signal and two real ultrasonic water turbulence noise were used to test the system performance and consistency. Results of all simulations and testing were discussed to improve the proposed system architecture.

IV. PROPOSED SYSTEM ARCHITECTURE

A. DATA ACQUISITION

In order to record the ultrasonic noise, it must be down-converted to the audible bandwidth, between 20 Hz and

TABLE 1. Comparison table with the existing systems to the proposed.

Leakage Detection Technology	Place of Application	Effective Scope	Sensitivity to Environmental Conditions	Portability
GPR	On the ground above the pipeline	Narrow (The cross-sectional area of the subsurface orthogonal to the surface)	Sensitive to moisture in soil	Portable
IR Camera	From tens of centimeters to a few of meters above ground	Wide (from tens of centimeters squared to several meters squared depending on the altitude)	–	Portable
THz Transducer	–	–	Sensitive to moisture in the tested material	Stationary
Conventional Offline Acoustic Detector	On the ground above the pipeline	Narrow (A few meters away from the acoustic sensor)	Affected by acoustic noise in the environment	Portable
Online Acoustic Detector	On the pipeline itself	Wide (Can cover a large-scale WDS depending on the number of sensors deployed)	Affected by acoustic noise in the environment	Portable
Proposed Offline Acoustic Detector	On the ground above the pipeline	Wide (Can cover a large-scale WDS depending on the number of sensors deployed)	Affected by acoustic noise in the environment	Portable

Information in this table is induced from the Literature Review, Introduction and models in their references, [1] – [14].

20 kHz, and then the frequency range of interest must be band-passed into several frames (20-40, 40-60, 60-80 and 80-100 kHz) which can be analyzed consequently by changing the shifting frequency used in down-conversion so that each ultrasonic bandwidth falls in the audible bandwidth at certain timeslot during the scanning process. A digital ultrasound to audio converter is already made [22]. It consists of a Microchip - dsPICFJ256GP710A microcontroller, one the fastest Microchip's processors with a sampling frequency that can reach 1.1 MHz and built-in 10-bit analog-to-digital converter (ADC), programmed to multiply the converted signal with a shifting frequency to attain an analog signal in the audible domain using a 20 pin digital-to-analog converter (DAC) at the end. To follow the aspects of this device, in the simulation of the proposed system the sampling frequency of processed signals will always be below 1.1 MHz. The upper limit of each band can be shifted to a frequency above 20 kHz and this is reachable where the typical sampling rate of recording devices is 44.1 kHz. Thus, the highest frequency that can be recorded according to Nyquist Theorem is 22.02 kHz.

B. AUDIO TRANSMISSION

The pre-processed acquired signals are transmitted over the cellular infrastructure as digitized data frames to a cloud storage instead of call voice sounds, where transmitting leakage noise data over voice calls seems inadequate for the following reasons. First, the bandwidth of voice calls transmitted through 2G and 3G technologies has lower bandwidth than the audible bandwidth (20 kHz). To be more precise,

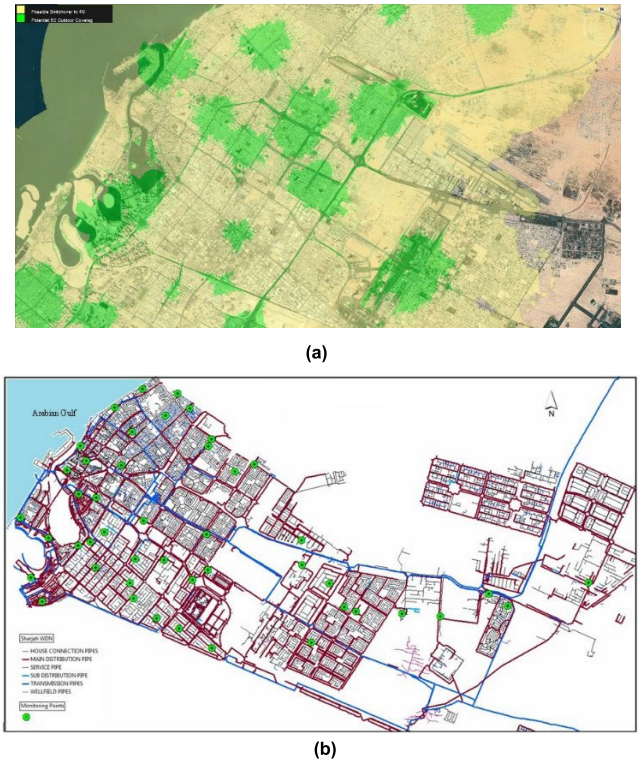

(a)

(b)

FIGURE 5. (a) Etisalat coverage areas for 4G network (green area) and 5G network (yellow area) coverage in Sharjah [25]. (b) WDN of SEWA where lines of different colors represent various kinds of pipes [26].

the voiceband of 2G networks ranges from 0.3 to 3.4 kHz, while 3G's HD Voice has a bandwidth between 50 Hz and 7 kHz. Thus, the scanned bandwidth must be divided into

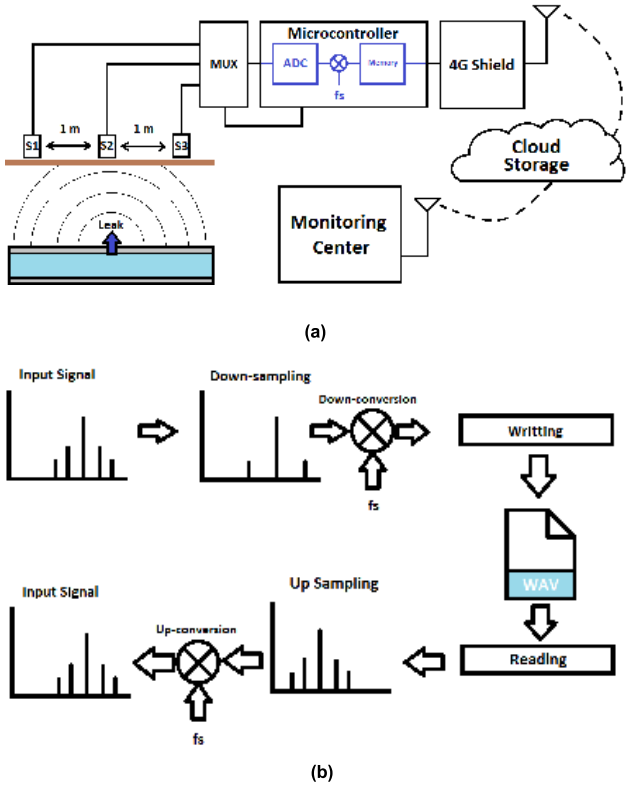

FIGURE 6. (a) Primary schematic of the proposed system. (b) Simplification of the primary schematic for simulation purposes.

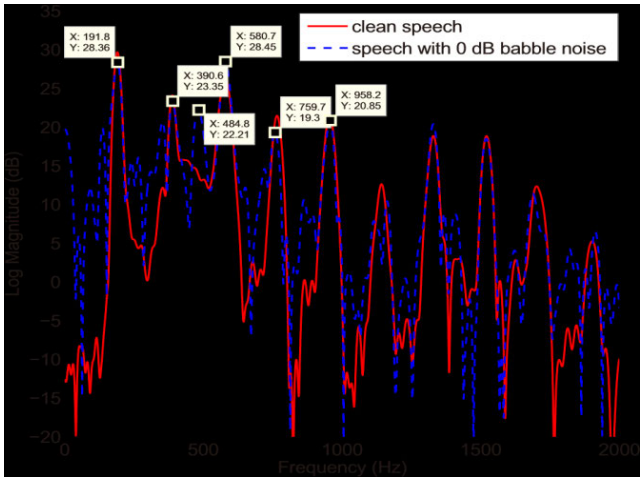

FIGURE 7. Spectrum of one frame of clean speech and speech with babble noise at 0 dB SNR [27].

larger number of frames increasing the repetitions of the down-conversion process and, in result, the power consumption which is a decisive point in electronics design. On the other hand, the bandwidth of the Full-HD Voice calls, a 4G technology firstly presented by Fraunhofer IIS, extends to 20 kHz [23]. However, the codec, coding and decoding processes, used in all cellular technologies compresses the audio before transmission, removing parts of the spectrum, according to the characteristics of the human sound perception and audiology. Difference between the nature of human sound

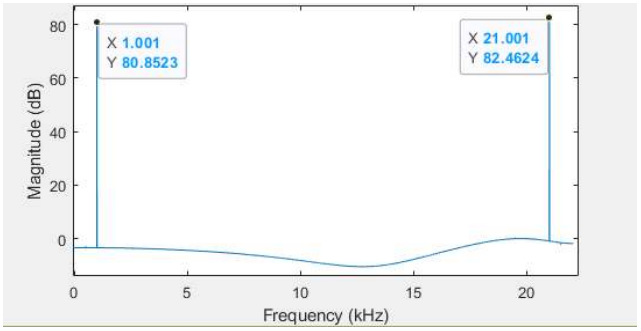

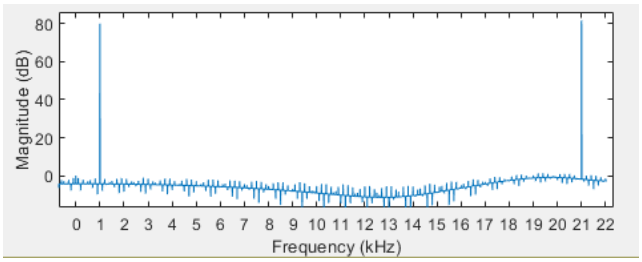

FIGURE 8. Spectrums of the down-converted frequency impulses originally at 80 and 100 kHz before and after the writing process shown in (a) and (b), respectively.

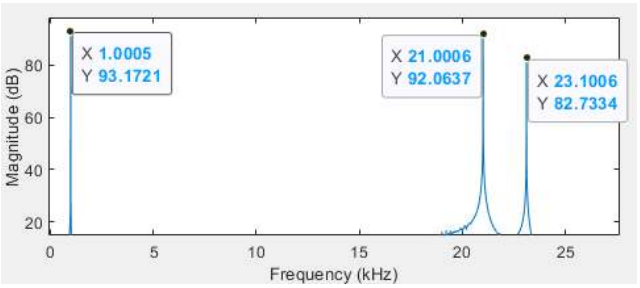

FIGURE 9. Frequency components of the interpolated signal.

and water turbulence noise can be noticed by comparing spectrums in Fig. 7, 11, 13, and 17. Therefore, a down-converted leakage noise, which has different characteristics, is not recommended to be transmitted through these telecommunication systems in fear of losing essential frequencies for detection process. The solution for this problem is to record the down-converted ultrasound as is in an uncompressed audio format and then upload as digitized data it to an online storage space from where the detector can retrieve it. A recorder with a sampling rate higher than 40 kHz, according to Nyquist Theorem, can record uncompressed raw audible waves in several file formats, such as WAV (Wave) and PCM (Pulse-code Modulation). A compressed audio file format, such as ADPCM (Adaptive Differential Pulse Code Modulation) cannot be used because it removes parts of the spectrum just like cellular technologies mentioned earlier. Several microcontrollers, such as Arduino, certain versions of PIC Microchip ...etc., can perform this task and upload the recording to the cloud storage via a communication shield. 5G cellular networks, which are already installed by the

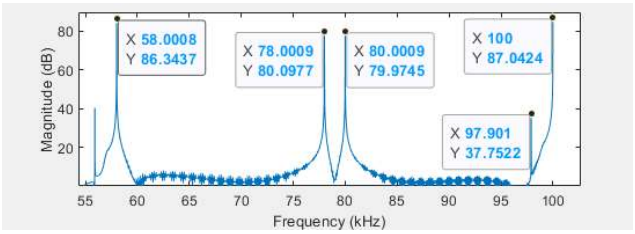

(a)

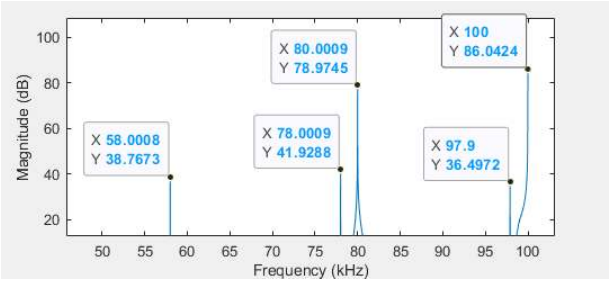

(b)

FIGURE 10. (a) Spectrum of the up-converted WAV file that passed through an Elliptic LPF with attenuation of 30 dB before being written. (b) Main components of the up-converted signal in (a) after passing through an HPF with attenuation level of 36.4 dB.

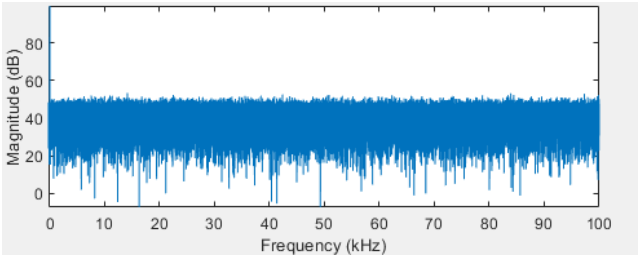

FIGURE 11. Noise spectrum of the simulated leakage noise signal.

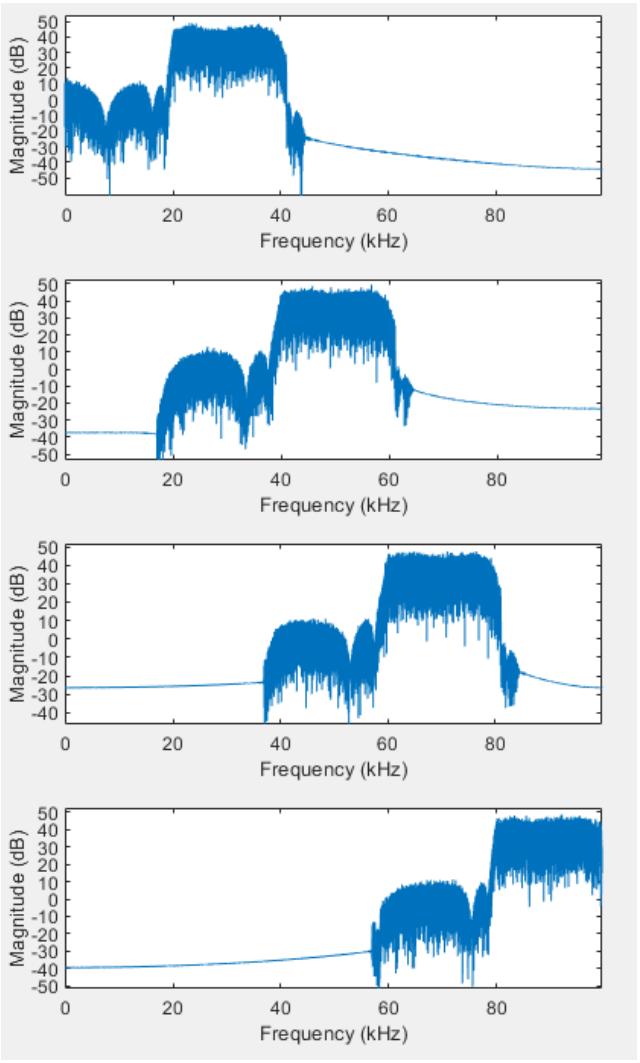

FIGURE 12. Spectrums of the output after inputting the frames (from up: 20-40, 40-60, 60-80, 80-100 kHz) band-passed from the random signal with the spectrum shown in Fig. 13.

Telecommunication Group Company, Etisalat, in the UAE, has an internet speed five times higher than that of the 4G services [24]. Yet, a few mobile devices are capable of accessing the 5G service at the mean time. Nevertheless, unlike the 4G networks, 5G networks' coverage is currently very limited, where the coverage map of Etisalat, see Fig. 5. 5G networks shows that this network cannot provide internet connection to sensors along the whole WDN of SEWA, nor at least along the main pipelines only. Thus, the 4G network is more reliable nowadays, but in westernmost area of Sharjah even using 3G network might is an inevitable option.

C. DATA ANALYSIS

Since the system will be monitoring a large number of points, a program must be written to automate the process of pinpointing a leakage which is done traditionally by observing the amplitude and frequency level indicators on the spectrum analyzer connected to the acoustic sensor or through headphones [19]. Several research papers offer algorithms for identifying the existence of a leakage through studying the spectrum of leakage noise [28], [29]. However, we will not go into the details of this process as the acoustic detectors that can perform it is widely commercially available. A multiplexer (MUX), controlled by the used microcontroller, can connect multiple sensors to the microcontroller. The schematic in Fig. 6 illustrates the components of the proposed system and its simplification of for simulation purposes. In the simulation, the upper sidebands after mixing processes and filtering will be discarded when necessary only if sidebands appeared in the bandwidth of interest in the spectrum. Note that the previous schematics do not include the filtering stages that will be added during the simulation because of different issues that will emerge in the coming sections.

V. RESULTS AND DISCUSSION

A. BOUNDARY TESTING

At the beginning of the simulation process, two impulses were generated at the ultrasonic frequencies, 80 and 100 kHz, to test the highest frame in the bandwidth of interest

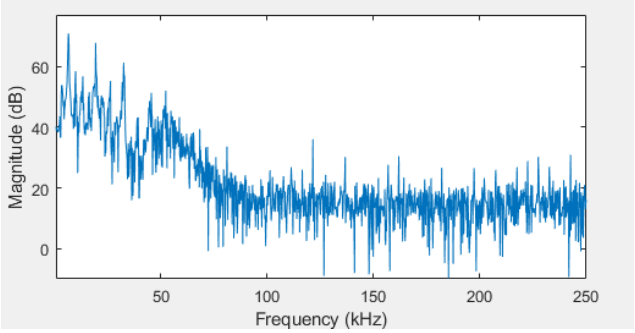

FIGURE 13. The spectrum of the first recorded real ultrasonic water turbulence noise.

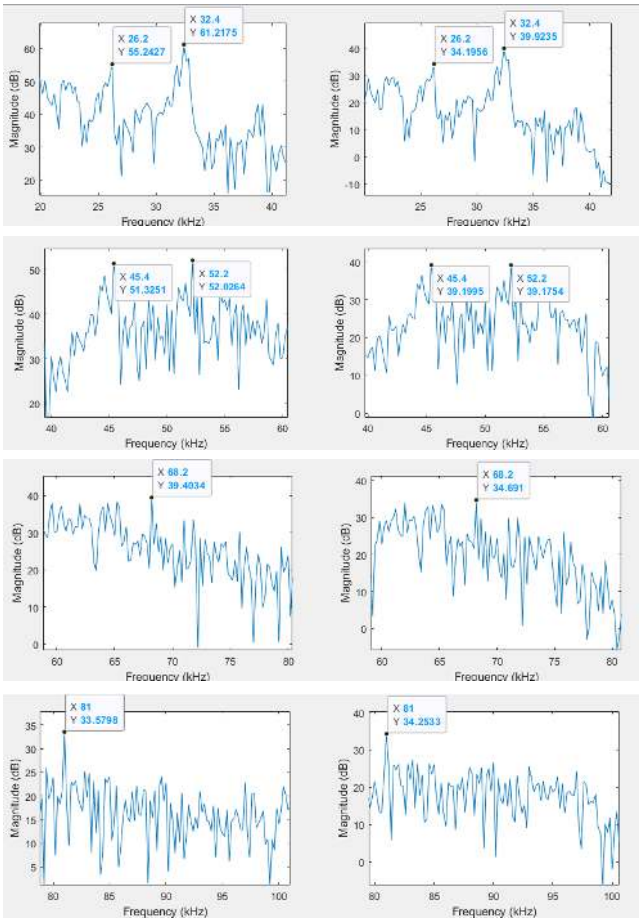

FIGURE 14. A zoomed in frames from the spectrum of the first recorded input signal are to the left while the resulting signal at the output of the network is to the right.

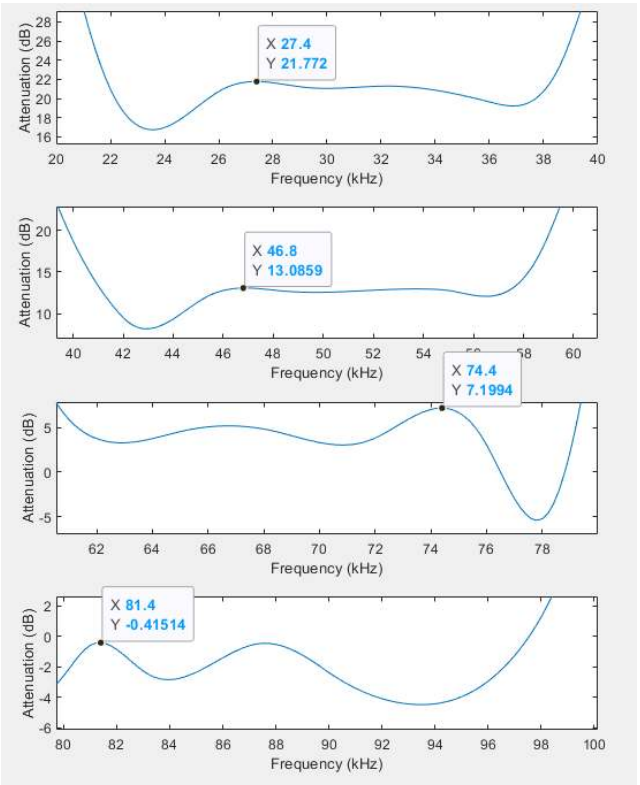

FIGURE 15. The difference between the upper peak envelopes of the spectrums of the first recorded input signal and that at the output after selecting the frames: 20-40, 40-60, 60-80 or 80-100 kHz, consequently from up. Each marker points at the absolute local maximum attenuation of the noise floor, or, in other words, the maximum difference between the envelope of the input and that of the output.

(20 to 100 kHz) at a sampling rate of 200kHz. This signal was modulated with a frequency of 79 kHz to down-convert it to the audible frequency to get the impulses at 21 and 1 kHz. Modulation was not with 80 kHz to avoid having the lower component at 0 Hz in the low-frequency noise range. Since a spur appeared at 41 kHz, it was filtered out with a sixth-order Butterworth low-pass filter (LPF) with a cutoff frequency of 22.05 kHz. This also removes other distortions that is not in the scope of interest, if any. The Butterworth filter was used since it has the no ripple in the pass-band region unlike other filters such as Chebyshev and Elliptic filters. The minimum difference between the magnitude of the spur at 41 kHz and magnitudes of other frequency component is 38.8 dB and this is acceptable as an audio signal with a spurious-free dynamic range (SFDR), the ratio of the fundamental signal to the strongest spurious signal in the output, equal to or above 30 dB is considered clean.

After that, the signal was down-sampled to have a sampling rate of 44.1 kHz, which is the typical sampling frequency of a recording device, to be written as a WAV audio file, a step that will be carried out by the microcontroller's ADC in the real system. The MATLAB function used for the sampling rate is ''resample,'' which incorporates an FIR anti-aliasing filter.

The spectrum of the written audio file, in Fig. 8, illustrates that the writing process resulted in low destortions below 0 dB level and a small attenuation in the input magnitude. Since the difference between the input frequencies and destortion level is 79 dB, above the minimum SFDR (30 dB), the signal is still considered clean. This shows that it is possible to transfer a down-converted ultrasonic noise signal in an acceptable accuracy from the sensing point to the analyzer in the format of WAV audio file. The audio file must be uploaded to a cloud

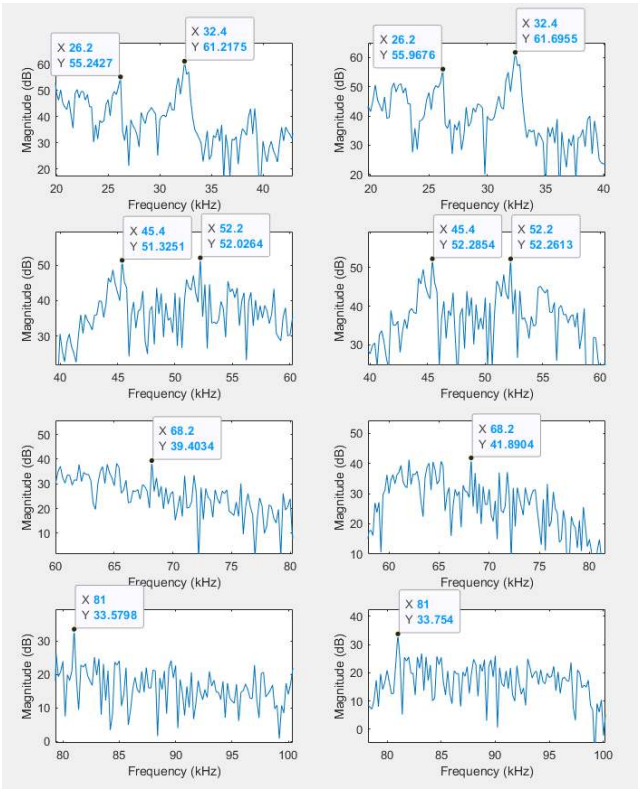

FIGURE 16. A zoomed in frames from the spectrum of the first recorded input signal are to the left while the retrieved signal at the output of the network after the addition of offsets is to the right.

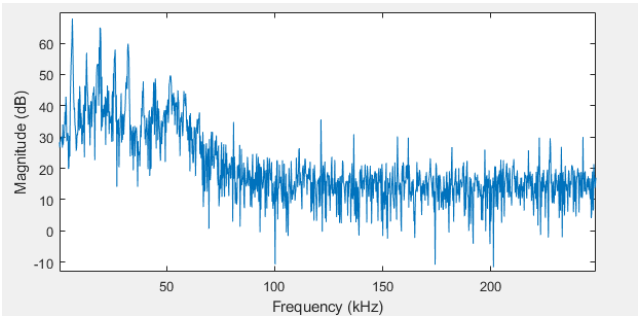

FIGURE 17. The spectrum of the second recorded real ultrasonic water turbulence noise.

storage that does not perform any compression (e.g. Google Drive) where some providers (e.g. Soundcloud) do compress files.

To feed the data into the anaylzer, the signal must return to its original bandwidth in the analog state for the acoustic detector to work conventially. Firstly, an interpolation is needed to increase the sampling frequency. Fig. 9 shows the frequency components of the WAV file after increasing its sampling frequency to 200 kHz. Although after the down-sampling the Butterworth LPF was effective in decreasing the frequency at 41 kHz to a level satisfactory for clean vocal signal condition, this time it is not as the resulting spur frequency is 23.1 kHz, closer to the down-converted input frequencies. As a result, it was replaced with a sixth-order

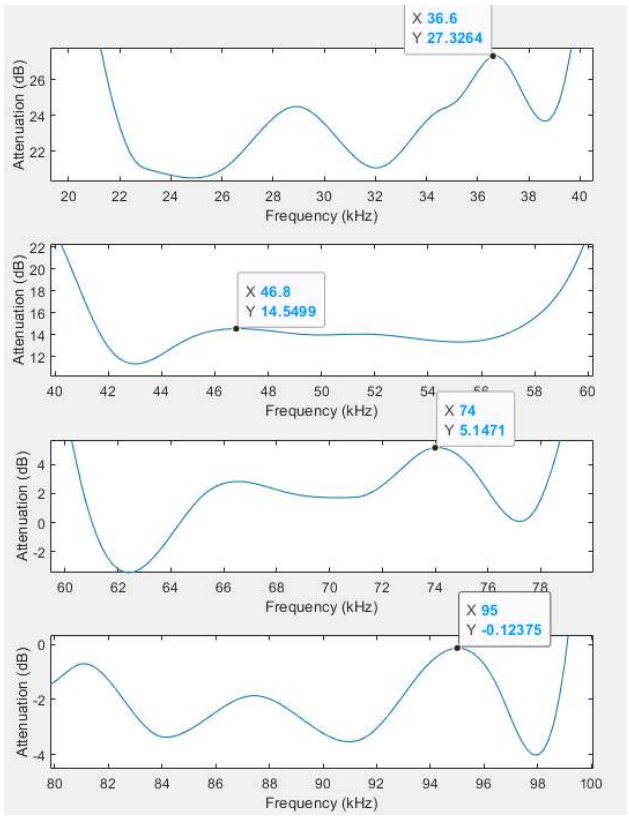

FIGURE 18. The difference between the upper peak envelopes of the spectrums of the second recorded input signal and that at the output after selecting the frames: 20-40, 40-60, 60-80 or 80-100 kHz, consequently from up. Each marker points at the absolute local maximum attenuation of the noise floor, or the difference between the envelope of the input and output.

Elliptic LPF with a peak-to-peak passband ripple of 1 dB and, consequently, a stopband attenuation of 30 dB. As the samples' number increased, the signal was up converted to its original bandwidth. Thus, the original frequencies, 80 and 100 kHz, were retrieved, but several other components were generated with significant magnitudes along with attenuation at 100 kHz as shown in Fig. 10 (a). Clearly, side components below 80 kHz can easily be filtered using a high-pass filter (HPF). However, in real-life the space between the boundary frequencies will be filled with possibly original frequencies making lossless filtering of components between 80 and 100 kHz, like the one at 97.9 kHz in this case, impossible under the imperfectness of stopband filters. To solve this issue, we manipulated the attenuation level of the Elliptic LPF between 22 and 100 kHz and found that a 30 dB attenuation is suitable to get the magnitude of 97.9 kHz 42.2 dB below the minimum of the two input frequencies. An Elliptic HPF, with an attenuation level of 36.4 dB and ripple of 1 dB, was used later to decrease the frequencies lower than 80 kHz 30 dB below the minimum input frequency as shown in Fig. 10 (b).

B. SIMULATED ULTRASONIC RANDOM NOISE TESTING

Now, the system was tested with a simulated leak noise signal. A leak noise can be modeled as a random signal [29].

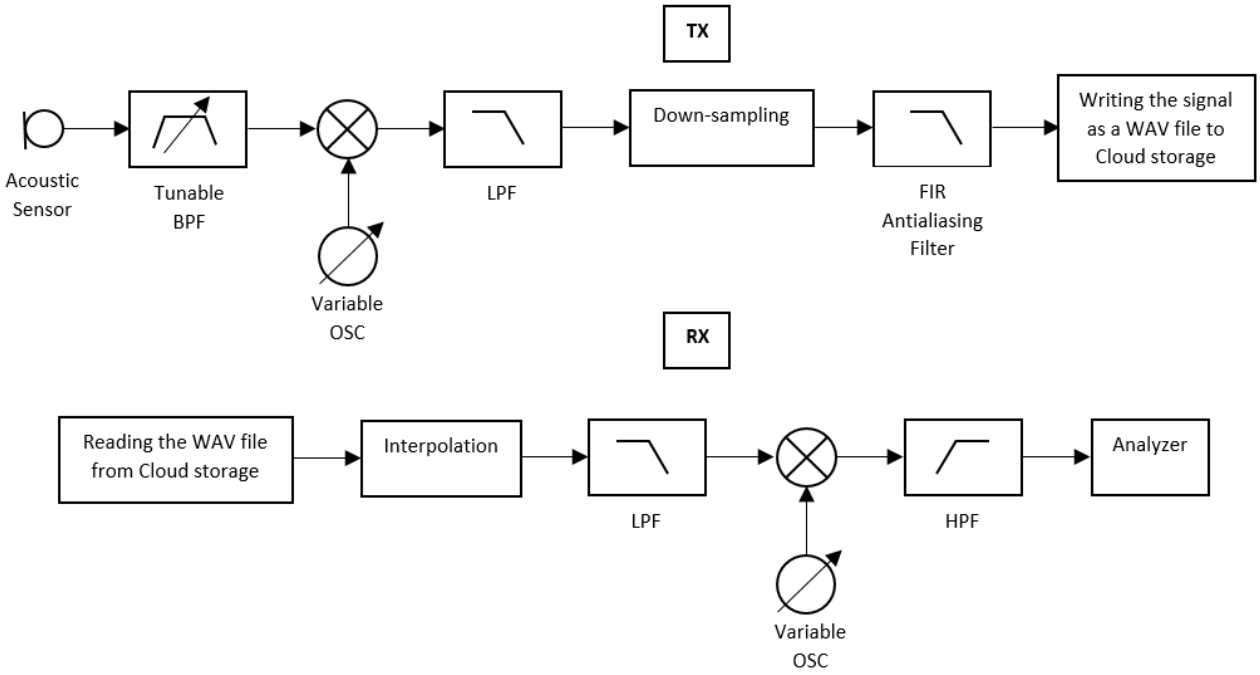

FIGURE 19. Final schematic of the proposed system with the transmitting side shown above, which is supposed to be in the field above the pipeline to be inspected, whereas the receiving side, which is supposed to be in the monitoring center, is shown below.

Although the magnitude of the noise floor is related to the depth of the leaking pipe, the shape of the breach in the pipe, the pressure of water inside and sensitivity of the sensor, arbitrarily, a random magnitude around 50 dB was chosen and the focus was getting the same level at the output. Fig. 11 shows the spectrum of the simulated input signal. Since the spectrum is continuous in this section, a sixth-order Butterworth band-pass filter was added at the beginning of the system to select the frame to be transmitted, 20-40, 40-60, 60-80 or 80-100 kHz. Spectrums, shown in Fig. 12, indicate that the output for each frame maintains a constant magnitude with a small varying attenuation around 4 dB. This attenuation probably resulted from writing the si gnal as during that process the signal must be normalized by its maximum value plus 0.1 to avoid clipping it.

C. REAL ULTRASONIC SIGNAL TESTING

In this section a real recording of ultrasonic water turbulence noise with a length of 5 ms and a sampling rate of 500 kHz was used as the input to the system. The ultrasonic turbulence noise was recorded from an ultrasonic cleaner using a Brüel & Kjær 8103 hydrophone connected to MATLAB via a Tektronix TDS 2002B oscilloscope. Fig. 13 shows the spectrum of the recorded ultrasonic noise where the decrease in the sensitivity of the transducer after 100 kHz is obvious. Fig. 14 shows a zoomed in frames from the spectrum in Fig. 13 opposite to the resulting signal at the output. As mentioned previously, the modulating signal in the down-conversion process and filters parameters where set in accordance with the boundaries of the frame to be down-converted. For example, to down-convert the frame, 20-40 kHz, it was mixed with a frequency of 19 kHz instead of 79 kHz after changing the cutoff frequencies of the selecting filter at the beginning to 20 and 40 kHz. Overall, the system was able to preserve the general shape of the spectrum of each frame. As shown in Fig. 14, the frequency with the absolute maximum value in addition to the difference between its magnitude and the level of adjacent noise were maintained except in the frame 40-60 kHz where two maximums had close values. However, the level of attenuation started to increase to considerable levels the more the frame was away from the frame upon which the system's parameters were set as explained in the subsection A of this section. Although the level of attenuation in a certain frame varies a little bit with frequency, most of frequencies tend to have close levels of attenuation. This can be better inspected by looking at the graphs in Fig. 15 which shows the difference between the upper peak envelopes of the spectrums of the input signal and that at the output in the bandwidths: 20-40, 40-60, 60-80 or 80-100 kHz, where the upper peak envelopes allow for measuring the noise floor level. Therefore, a constant gain can be added to offset the attenuation in each frame. Fig. 16 shows the selected input bandwidths and the retrieved output with the offsets equal to the local maximum attenuation in each frame according to Fig. 15. To ensure the consistent performance of this solution, the difference between the envelopes of the input and output for a second ultrasonic noise recording, with the spectrum shown in Fig. 17, was measured and found to have similar levels of attenuation in all frames like the first recorded ultrasonic input as shown in Fig. 18. The attenuation levels for the second input can be compared to attenuation levels in Fig. 15. After solving the attenuation

problem at the output of the network, the signal can be fed into the analyzer which can work according to various algorithms or strategies. The preservation of the shape of the spectrum and recovery of the magnitude of its components allows the analyzer to work probably because many leakage detection strategies and algorithms usually depends on the recognition of the amplitude of the leak noise [17], [28], [29], [31], [32]. Fig. 19 shows the final schematic of the communication system with all filters added.

VI. CONCLUSION

This paper introduces a 4G communication system for ultrasonic leakage detectors that can fit between the ultrasonic transducer and the analyzer allowing multiple inputs into a single analyzer without changing the structure or programming of the analyzer itself. The system uses band-passing, down-conversion and then down-sampling in order to cut an input random wave from an acoustic transducer into four frequency frames (20-40, 40-60, 60-80 or 80-100 kHz) and then record each frame into an uncompressed audio. On the analyzer side, each WAV file is up-sampled and then up-converted with an Elliptic HPF cascaded with a Butterworth HPF to have an output with an SFDR of at least 30 dB which represent part of the original signal to be analyzed for leakage detection. A simulation was done to validate the proposed system operation in ideal conditions where leakage noise has a constant magnitude over all frequencies. Results proved the system's ability to preserve the shape of noise with a small attenuation around 4 dB. However, when a real ultrasonic water turbulence noise signals were input, the level of attenuation started to increase to considerable levels the more the frame was away from the frame upon which the system's parameters were set. Because the level of attenuation varied a bit in each frame, a constant gain could be added to each frame according to its maximum level of attenuation. Although this solution seemed appropriate for different real signals, in future studies we will consider using deconvolution as it is expected to apply evenly to all frequencies in a frame unlike the proposed solution. Finally, since in field noise is expected to come from different environmental sources mentioned earlier in the introduction, in future studies, we will focus more in denoising techniques as well.

REFERENCES

[1] D. Ayala-Cabrera, E. Campbell, E. Carreño-Alvarado, J. Izquierdo, and R. Pérez-García, "Water leakage evolution based on GPR interpretations," *Procedia Eng.*, vol. 89, pp. 304–310, Jan. 2014.

[2] M. Stone. (2002). *Gemstone Exploration Techniques—Ganoksin Jewelry Making Community*. Accessed: Aug. 9, 2019. [Online]. Available: https://www.ganoksin.com/article/gemstone-exploration-techniques/

[3] B. Shakmak and A. Al-Habaibeh, "Detection of water leakage in buried pipes using infrared technology; A comparative study of using high and low resolution infrared cameras for evaluating distant remote detection," in *Proc. AEECT*, Dead Sea, Jordan, 2015, pp. 202–296.

[4] J. F. Federici, "Review of moisture and liquid detection and mapping using terahertz imaging," *J. Infr., Millim., THz Waves*, vol. 33, no. 2, pp. 97–126, 2012.

[5] Z. Wang, M. Hu, E. E. Kuruoglu, W. Zhu, and G. Zhai, "How do detected objects affect the noise distribution of terahertz security images?" *IEEE Access*, vol. 6, pp. 41087–41092, 2018.

[6] T. Tanabe, T. Kanai, K. Kuroo, T. Nishiwaki, and Y. Oyama, "Non-contact terahertz inspection of water content in concrete of infrastructure buildings," *World J. Eng. Technol.*, vol. 6, no. 2, pp. 275–281, 2018.

[7] Emerging Technology from the arXiv, MIT Technology Review. (Apr. 10, 2019). *A Revolutionary Imaging Technique Uses a Single Pixel to Fill Our Terahertz Blind Spot*. Accessed: Nov. 13, 2019. [Online]. Available: https://www.technologyreview.com/s/613278/a-revolutionary-imaging-technique-uses-a-single-pixel-to-fill-our-terahertz-blind-spot/

[8] *Terahertz Air-Coupled Time Domain Measurement Kit (ACMK-F)*. Accessed: Aug. 17, 2019. [Online]. Available: https://www.terahertzstore.com/products/terahertz-measurement-kits/air-coupled-time-domain-measurement-kit-acmk-f.htm

[9] J. H. Moore and N. D. Spencer, "Fundamentals," in *Encyclopedia of Chemical Physics and Physical Chemistry*. Bristol, U.K.: Institute of Physics Publishing, 2001, p. 1063.

[10] A. Al Hawari, M. Khader, T. Zayed, and O. Moselhi, "Detection of leaks in water mains using ground penetrating radar," *Int. Scholarly Sci. Res. Innov.*, vol. 10, no. 4, pp. 422–425, 2016.

[11] FLIR. *sUAS Cameras & Kits*. Accessed: Dec. 22, 2018. [Online]. Available: https://www.flir.com/browse/home-amp-outdoor/drone-cameras/

[12] *Underground Water Leak Detection*. Accessed: Sep. 13, 2019. [Online]. Available: https://tsienergysolutions.com/leak-detection/

[13] Q. Yang, Y. Zeng, Y. Zhang, H. Wang, B. Deng, and Y. Qin, "Envelope correction of micro-motion targets based on multi-layer perceptron during THz-ISAR sensing," *IEEE Access*, vol. 7, pp. 183596–183603, 2019.

[14] J.-P. Guillet, B. Recur, L. Frédérique, B. Bousquet, L. Canioni, I. Manek-Hönninger, P. Desbarats, and P. Mounaix, "Review of terahertz tomography techniques," *J. Infr., Millim., THz Waves*, vol. 35, no. 4, pp. 382–411, Apr. 2014.

[15] A. S. Bandes, "Detecting underground leaks with ultrasonics," *Maintenance J.*, vol. 18, no. 3, 2000.

[16] M. R. Holcomb, S. N. Schneider, and J. F. Briggs, "100 kHz bandwidth ultrasonic recording system," *Instrum. Sci. Technol.*, vol. 43, no. 2, pp. 214–221, Jan. 2015.

[17] *Scottish Water Adopts New Phocus3 Acoustic Noise Logging for Effective Leak Location*. Accessed: Aug. 3, 2019. [Online]. Available: https://www.primayer.com/wp-content/uploads/2018/04/Phocus3-Scottish-Water-Case-Study-CS1-PH3-044-2.0.pdf

[18] PQWTCS. (Sep. 9, 2017). *Operation Video for 2017 Latest Water Leak Detector PQWT CL Series [Video File]*. [Online]. Available: https://www.youtube.com/watch?v=skKHUHIFcJU

[19] S. Ravi, P. Dodorico, T. M. Over, and T. M. Zobeck, "On the effect of air humidity on soil susceptibility to wind erosion: The case of air-dry soils," *Geophys. Res. Lett.*, vol. 31, no. 9, 2004, Art. no. L09501.

[20] H. Dajani. (Jul. 15, 2019). UAE Weather: Humidity Up to 85 Per Cent. The National. Accessed: Aug. 10, 2019. [Online]. Available: https://www.thenational.ae/uae/environment/uae-weather-humidity-up-to-85-per-cent-1.886270

[21] M. L. Oelze, W. D. O'Brien, and R. G. Darmody, "Measurement of attenuation and speed of sound in soils," *Soil Sci. Soc. Amer.*, vol. 66, no. 3, May, pp. 788–796, 2002.

[22] T. Fredriks. (2010). Ultrasonic Listener: Microcontroller Based Frequency Shifter. Digital Commons at Cal Poly. Accessed: Aug. 7, 2019. [Online]. Available: http://digitalcommons.calpoly.edu/cgi/viewcontent.cgi?article=1047&context=eesp

[23] T. Fredriks. (2010). Ultrasonic Listener: Microcontroller Based Frequency Shifter. Digital Commons at Cal Poly. Accessed: Aug. 7, 2019. [Online]. Available: http://digitalcommons.calpoly.edu/cgi/viewcontent.cgi?article=1047&context=eesp

[24] Khaleej Times. (Jun. 1, 2019). *No Extra Charges for 5G in UAE*. [Online]. Available: https://www.khaleejtimes.com/business/telecom/No-extra-charges-for-5G-in-UAE-

[25] *Etisalat*. Accessed: Sep. 10, 2019. [Online]. Available: https://www.etisalat.ae/en/system/wst/assets/img/consumer/5g/sharja.jpg

[26] M. M. Mortula, T. A. Ali, R. Sadiq, A. Idris, and A. A. Mulla, "Impacts of water quality on the spatiotemporal susceptibility of water distribution systems," *CLEAN-Soil, Air, Water*, vol. 47, no. 5, 2019, Art. no. 1800247.

[27] N. Yang, H. Ba, W. Cai, I. Demirkol, and W. Heinzelman, "BaNa: A noise resilient fundamental frequency detection algorithm for speech and music," *IEEE/ACM Trans. Audio, Speech, Language Process.*, vol. 22, no. 2, Dec., pp. 184–1833, Aug. 2014.

[28] S. Liu, L. Li, J. Cui, and T. Li, "Acoustic emission detection of underground pipeline leakage," in *Proc. 15th WCNDT*, Rome, Italy, 2000.

[29] M. S. El-Abbasy, F. Mosleh, A. Senouci, T. Zayed, and H. Al-Derham, "Locating leaks in water mains using noise loggers," *J. Infrastruct. Syst.*, vol. 22, no. 3, 2016, Art. no. 04016012.
[30] D.-B. Yoon, J.-H. Park, and S.-H. Shin, "Improvement of cross-correlation technique for leak detection of a buried pipe in a tonal noisy environment," *Nucl. Eng. Technol.*, vol. 44, no. 8, pp. 977–984, Dec. 2012.
[31] A. Martini, M. Troncossi, and A. Rivola, "Leak detection in water-filled small-diameter polyethylene pipes by means of acoustic emission measurements," *Appl. Sci.*, vol. 7, no. 2, Dec. 2016.
[32] *LD6000 Combination Detector for Leak Detection—TROTEC*. Accessed: Aug. 9, 2019. [Online]. Available: https://uk.trotec.com/products-services/measuring-devices/leak-detection/combination-measuring-devices-for-leak-detection/ld6000-combination-detector-for-leak-detection/

AMEEN AWWAD received the B.Sc. degree from the American University of Sharjah (AUS), in 2019. He is currently a Researcher with the Electrical Engineering Department, AUS.

MOHAMED YAHYIA received the B.Sc. degree from the Higher School of Sciences and Health Techniques, Tunis, Tunisia, in 2000, the M.Sc. degree from the Higher School of Communication, Tunis, in 2002, the Ph.D. degree in telecommunication engineering conjointly from the National Engineering School of Gabes (NESG), Tunisia, and the Ecole Nationale Supérieure d'Electrotechnique, d'Electronique, d'Informatique, d'Hydraulique et des Télé communications (ENSEEIHT), Toulouse, France, in 2010, and the Habilitation degree in telecommunications from the University of Gabés, Tunisia, in 2017.

Since 2018, he has been an Associate Professor with NESG. Since 2019, he has also been a Postdoctoral Research Associate with the American University of Sharjah. His current research interests include analysis of polarimetric SAR images and numerical methods in electromagnetism.

LUTFI ALBASHA received the B.Eng. and Ph.D. degrees in electronic and electrical engineering from the University of Leeds, U.K. In 1997, he joined Sony Corporation, where he was involved in commercial RFIC chip products for mobile handsets. In 2000, he joined Filtronic Semiconductors, as a Senior Principal Engineer, where he created an IC Design Team. The team supported the company foundry design enablement for mass production of RFIC products and taped-out its first commercial chips. This becomes a very successful business in Europe's largest GaAs MMIC foundry. He returned to Sony as a Lead Principal Engineer, where he was involved in highly integrated RFCMOS and BiCMOS transceivers for cellular and TV applications. He joined the American University of Sharjah, where he is currently a Professor with the Electrical Engineering Department. His current areas of research are in energy harvesting and wireless power transfer, low-power implantable devices, power amplifier design and linearization, and integrated digital radar transceivers. He has received several outstanding recognition awards from Sony Corporation, the IET, the IEEE, and the University of Leeds. He is an Associate Editor of the *IET Microwaves, Antenna and Propagation Journal*. He has served for three years as the President of the UAE Chapter of the IEEE Solid-State Circuits Society.

MD. MARUF MORTULA received the B.Sc. degree with the Bangladesh University of Engineering and Technology, Bangladesh, in 2000, and the M.Sc. and Ph.D. degrees with Dalhousie University, Halifax, NS, Canada, in 2002 and 2006, respectively. Since 2018, he has been a Full Professor with the American University of Sharjah. His research interests include water and wastewater treatment, recycling of solid waste management, water quality management in coastal water, and water infrastructure management.

TARIG ALI received the B.S. degree (Hons.) in civil engineering from the University of Khartoum, Sudan, in 1993, and the M.S. and Ph.D. degrees from The Ohio State University, USA, in 1999 and 2003, respectively. He is currently an Associate Professor with the American University of Sharjah. His research areas include geospatial engineering, GIScience, coastal mapping & GIS, and applications of GIS and remote sensing in civil and environmental engineering.